BNWL-339

2-

AEC RESEARCH and DEVELOPMENT REPORT

DOSIMETRY TECHNOLOGY STUDIES

DOSIMETRY TECHNOLOGY STAFF

NOVEMBER, 1966

BATTELLE-NORTHWEST
BATTELLE MEMORIAL INSTITUTE / PACIFIC NORTHWEST LABORATORY

LEGAL NOTICE

PACIFIC NORTHWEST LABORATORY
RICHLAND, WASHINGTON
operated by
BATTELLE MEMORIAL INSTITUTE
for the
UNITED STATES ATOMIC ENERGY COMMISSION UNDER CONTRACT AT(45-1)-1830

PRINTED BY/FOR THE U. S. ATOMIC ENERGY COMMISSION

AEC-RLOO RICHLAND, WASH.

BNWL-339
UC-48, Biology and
Medicine

DOSIMETRY TECHNOLOGY STUDIES
-1965-

By

Dosimetry Technology Staff

Environmental Health and Engineering Department

November 1966

PACIFIC NORTHWEST LABORATORY
RICHLAND, WASHINGTON

Printed in USA. Price $2.00. Available from the
Clearinghouse for Federal Scientific and Technical Information
National Bureau of Standards
U.S. Department of Commerce
Springfield, Virginia

CONTENTS

LIST OF FIGURES

LIST OF TABLES

DOSIMETRY TECHNOLOGY STUDIES
—1965—

THERMOLUMINESCENT DOSIMETRY STUDIES

G. W. R. Endres

INTRODUCTION

The property of thermoluminescence can be used to determine radiation dose. Studies of several materials--LiF, CaF_2 and Ca_2SO_4--with appropriate activators were considered for special dosimetry applications and for replacements for film badge dosimeters and finger ring dosimeter. The use of LiF as a neutron dosimeter in place of NTA film in personnel neutron dosimeters is of particular interest. Battelle-Northwest studies have concentrated on the application of LiF to gamma, X-ray, neutron and beta dosimetry for personnel monitoring.

GAMMA AND X-RAY DOSIMETRY

Thermoluminescence response to various gamma and X-ray energies and radiation exposures was investigated for two types of powdered LiF--A and B--supplied by two manufacturers. Unless otherwise specified, powder A was used for all the experiments detailed here. Small teflon cylindrical dosimeter capsules in groups of five containing powder A were exposed to 100, 200, and 300 mR of monoenergetic radiation at energies of 16, 23, 34, 58 and 100 keV, and about 1250 keV (^{60}Co). Powder B received the same three exposures at X-ray energies of 16, 34, and 100 keV, and 1250 keV (^{60}Co). The light emitted in the first readout was found to be proportional to the radiation exposure for both powders. Figure 1 illustrates this for powder A (the response of powder A was observed to be twice as large as that of powder B). A different shipment of powder A was also given exposures of 50 to 1000 mR; again, the response versus exposure was essentially linear, as shown in Figure 2. In Figure 3, the sensitivity, measured in arbitrary light-output units per mR, is plotted versus gamma or X-ray energy for powder A. The 95% confidence limits were calculated for the energy response data, based on five measurements at each data point. The uncertainties varied from ±3% to ±8% and averaged ±5%.

Screened capsules were studied briefly in an attempt to minimize the already low energy dependence. The small screens used were intended to reduce the excess sensitivity at low energies; however, it was found that the peak was replaced by a dip in the energy response curve. At 8 keV, the response was approximately one-third of that at 100 keV. The screen did not improve the energy response, but merely changed the response.

The relationship between the light emitted and the amount of powder present in the heating element was studied for the thermoluminescent reader currently in use by exposing dosimeters, in groups of five containing 25, 50, 75, 100, and 125 mg of LiF, to 500 mR of radium-gamma radiation. The light emitted in the first readout was proportional to the powder

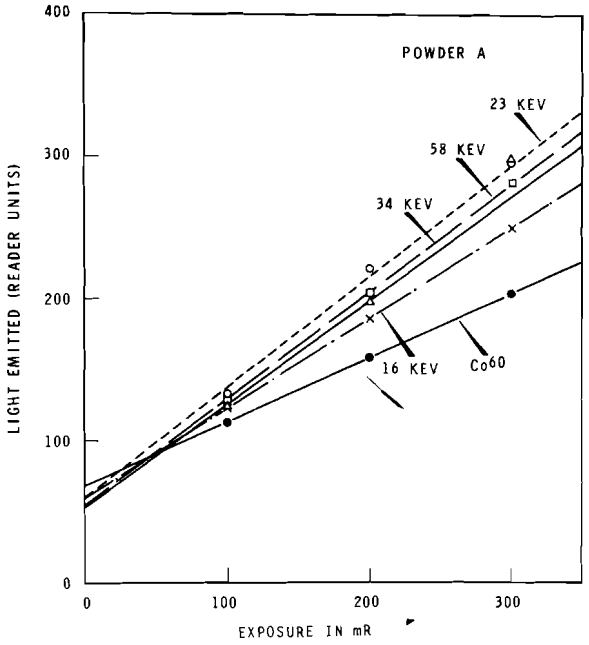

FIGURE 1. Calibration Curve for 16, 23, 34, 58, and 100 keV X-Rays and ^{60}Co Gamma Rays

weight for 25 and 50 mg, reached a maximum at 100 mg, and then decreased. (See Figure 4.) When the planchet contains too much powder, that on top may not get hot enough to free the trapped electrons; thus, not only does it not luminesce, but also it absorbs some of the light emitted by the powder closer to the planchet. Figure 5 illustrates the magnitude of this effect, in reader units per milligram of LiF, for one commercial reader geometry.

As indicated earlier, there was a pronounced difference in sensitivity between powders A and B from the two manufacturers. Similar variations were also observed between different shipments of powder from the same company. Moreover, the same powder

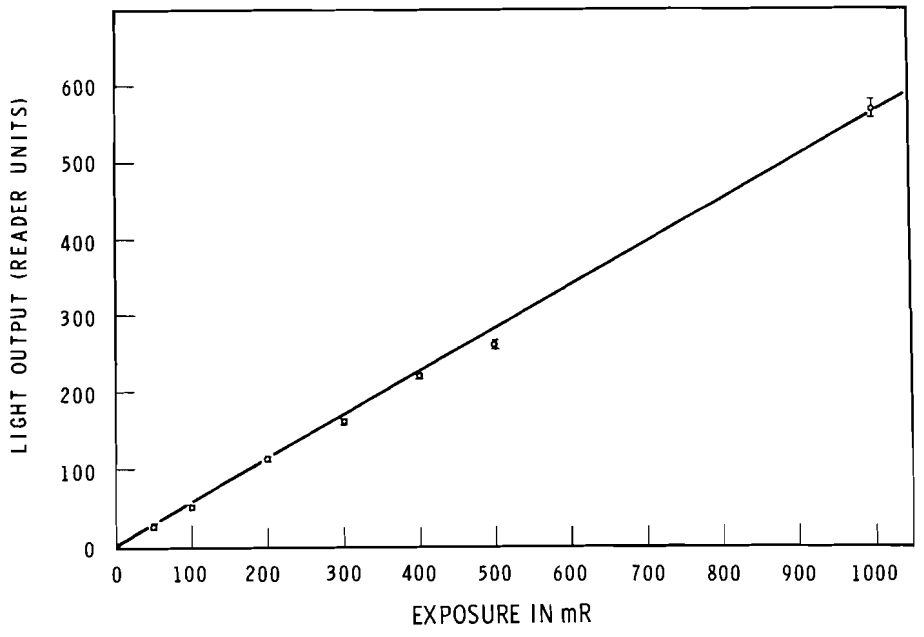

FIGURE 2. Calibration Curve for 100 keV X-Rays

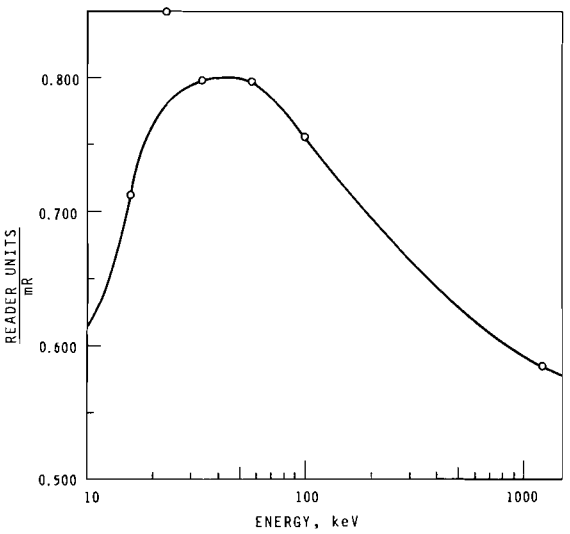

FIGURE 3. Photon Energy Dependence of Thermoluminescent Dosimeters

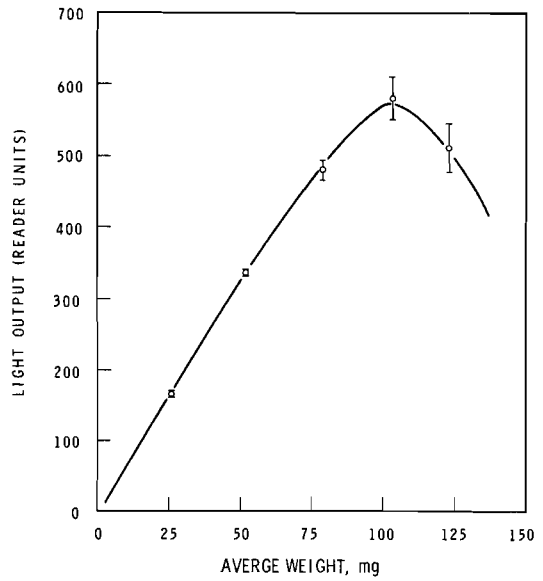

FIGURE 4. Dependence of Light Emitted on Amount of Powder Present

varied in sensitivity depending upon its previous thermal and radiation history. Table I shows the results of experiments in which each dosimeter was exposed to 500 mR of ^{60}Co γ-radiation. For example, in the

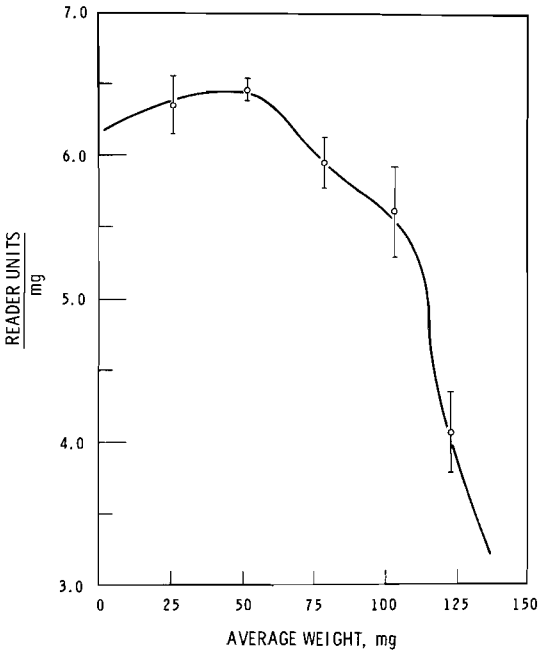

FIGURE 5. Weight Sensitivity of LiF

fifth row, powder A (third shipment) was exposed without prior annealing, readout, annealed, exposed again to 500 mR, and finally read out, yielding a reading of 400 reader units. The data in rows one and two indicate that annealing the powder (1 hr at 400 °C plus 24 hr at 80 °C), before using it the first time, increases the sensitivity. Powder that was used before, but not annealed, gives the highest readings. This may be due to some activated electrons remaining in the deeper electron traps and not returned to the ground state in the first reading. More consistent results may be obtained by always annealing the powder after using it to insure the complete emptying of all traps.

To determine the influence of particle size, the LiF powder was sieved

TABLE I. Relationship Between LiF Phosphor History and Light Emission from 500 mR ^{60}Co Gamma-Ray Exposure

LiF Powder	History	Light Emitted Reader Units
A	(new)	240
A	(new, annealed[+])	329
A	(new, used[*])	373
A	(new, used, annealed)	357
A	(new, used, annealed, used)	401
B	(new)	168

[+] *The annealing procedure consisted of baking the LiF at 400 °C for 1 hr followed by 24 hr at 80 °C.*

[*] *"used" indicates the LiF was exposed to γ rays and the thermoluminescence read out prior to the 500 mR exposure.*

between screens of 100 mesh (149 μ and 200 mesh (74 μ). The powder with grain sizes in the 74 to 149 μ range, and that >149 μ, were exposed to 500 mR of radium-gamma radiation, and the dose response compared. The difference in response per 50 mg sample was found to be less than 5%; therefore, particle size in this rather narrow range is a relatively unimportant parameter for radium-gamma radiation exposures. The effect of grain size on neutron dose sensitivity remains to be investigated.

To function as a satisfactory dosimeter, the thermoluminescent powder should have a response which is independent of the storage time (at room temperature) between exposure and readout. To investigate this property, 35 dosimeters, in seven groups of five each, were exposed simultaneously to 300 mR, stored at room temperature, and the groups read out at various times during the next 15 days. At the end of that time the light emitted was 95% of the quantity emitted after the first day, Figure 6. Heating the exposed powder to 80 °C for 1 hr also resulted in about a 5% decrease in the quantity of light emitted. The uncertainties calculated for these data are less than ±2% based on 95% confidence limits.

NEUTRON DOSIMETRY IN THE PRESENCE OF GAMMA RADIATION

Since neutron radiations are usually accompanied by gamma radiation, a neutron dosimeter should either be insensitive to gamma rays or should be capable of separating the neutron component of the dose from that contributed by gamma rays. The neutron dosimeter which was studied consists of two vials filled with LiF powder. One vial contains only LiF, and is intended to respond to the gamma radiation only. The direct fast-neutron response of LiF is small, and may be assumed to be negligible in these studies. The other vial contains the same amount of LiF, but the voids between the grains are filled with ethyl alcohol (C_2H_6O). The fast neutrons collide with the hydrogen nuclei and project energetic recoil protons into the LiF grains, thus giving rise to an indirect fast-neutron response. When the reading of the "dry" (LiF only) vial is subtracted from that of the "wet" (LiF + alcohol) vial, a difference reading proportional to the fast-neutron dose should be obtained. The process is illustrated schematically in Figure 7.

It cannot be assumed a priori that the gamma ray response of the wet dosimeter will be the same as that of the dry dosimeter. The relative

response of pairs of wet and dry LiF dosimeters receiving equal exposures over the photon energy range from 16 keV to 1.25 MeV was measured yielding the results shown in the lower two curves of Figure 8. While the wet and dry dosimeters agree at 1.25 MeV (^{60}Co gamma radiation), the wet dosimeter tends to give a lower response than the dry dosimeter for photon energies of 100 keV and below. At 26 keV the wet dosimeter response is lower by about 14%. This photon energy-dependence of the wet-to-dry dosimeter response ratio implies that, for optimizing the accuracy of neutron dosimetry by this method, some knowledge of the energy spectrum of the gamma radiation present in the mixed neutron and gamma radiation field is required.

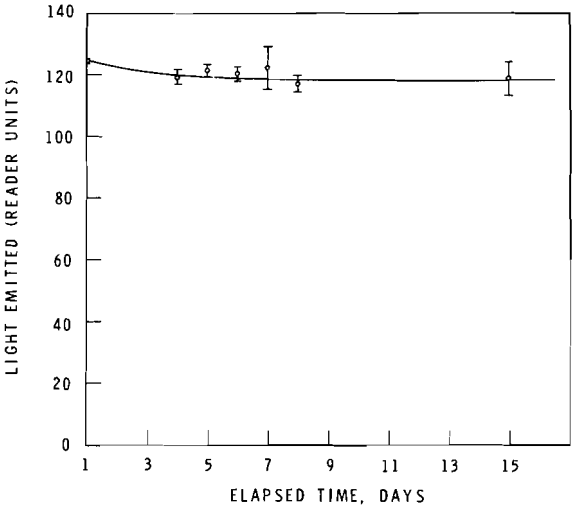

FIGURE 6. Stability of LiF over a 15 Day Period

Clearly, it would be an advantage if the two dosimeters exhibited identical gamma radiation response over the entire energy range of interest. An apparent approach is the filling of the "dry" dosimeter with a non-hydrogenous fluid which has the same influence on the gamma ray response

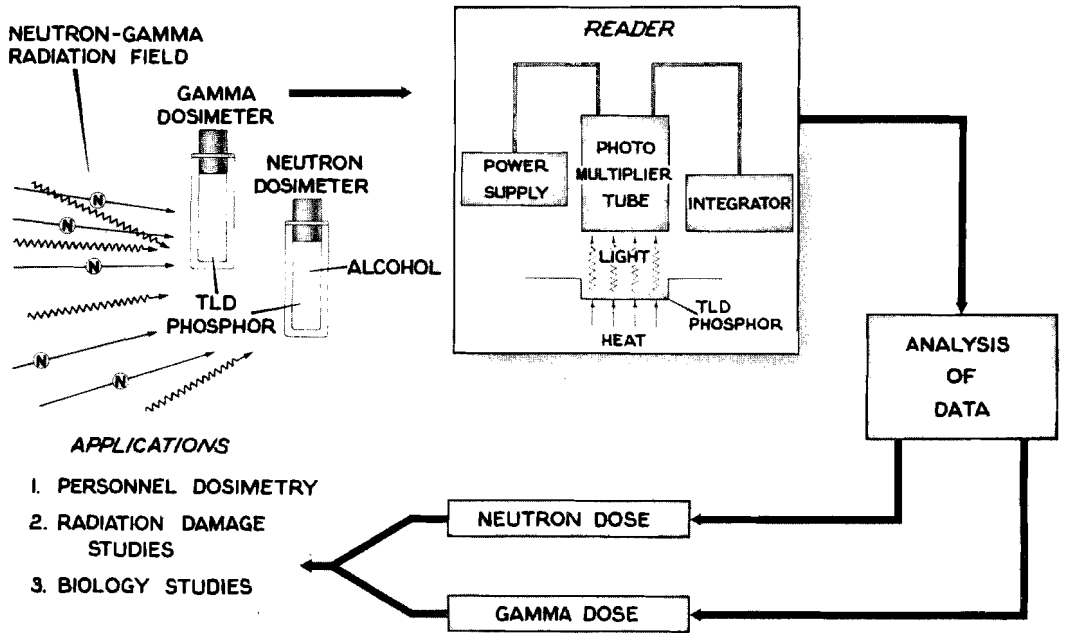

FIGURE 7. Thermoluminescent Dosimeters

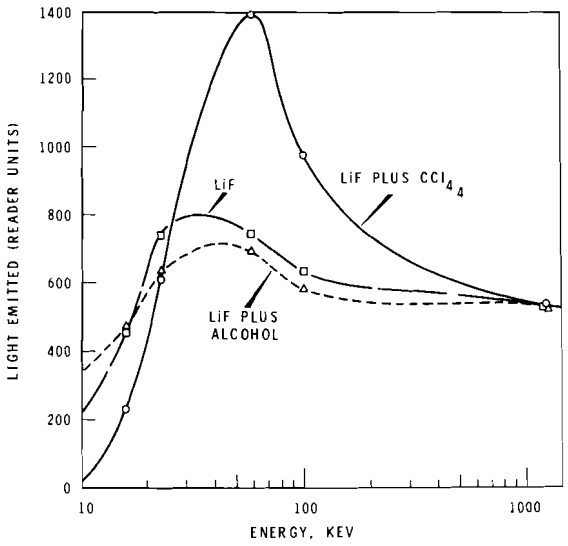

FIGURE 8. Photon Energy Dependence of Thermoluminescent Neutron Dosimeters

as ethyl alcohol. CCl_4 was investigated (see upper curve in Figure 8), but evidently the photoelectric effect of chlorine causes too much enhancement of the response at low energies. This approach produced substantial increases in photon energy response. At 60 keV it increased the photon response by a factor of two. Under certain conditions, this may be useful for providing a lowering of the LiF detection limit in this energy range.

As a preliminary test of the effectiveness of ethyl alcohol filling for detecting fast neutrons with LiF dosimeters, a series of exposures of wet versus dry dosimeters was performed with PuF_4 and PuBe neutron sources. The average neutron energy from the PuF_4 source was about 0.8 MeV; that from the PuBe source was about 4.5 MeV. Both sources also emitted gamma radiation; PuF_4 had the greater gamma radiation exposure rate. The resulting thermoluminescence readings are given in Table II.

It is evident from these preliminary data that the response is not linear with the dose; the cause of this is not known at the present time. Nevertheless, from the similarity (within ±6%) of the wet and dry dosimeter readings at corresponding doses

TABLE II. Neutron Exposures

Neutron Exposure in rads	Average Reading Dry LiF	Average Reading LiF + Alcohol	Δ Reading rad
	PuF_4 Source		
(5.4×10^7 n/cm^2/rad*)			
0.1	252	237	-150
0.2	356	340	- 80
0.3	655	686	+100
	PuBe Source		
(3.3×10^7 n/cm^2/rad*)			
0.1	34	41	+ 70
0.4	77	95	+ 45
0.8	167	211	+ 55

1st collision dose--(rads) at average energy NBS Handbook 63 for PuF_4--0.8 MeV PuBe--4.5 MeV

from the PuF_4 source, it is evident that the alcohol-filling technique is incapable of producing a significant enhancement of fast-neutron sensitivity for 0.8 MeV neutrons in the presence of a relatively large gamma radiation exposure. The results with the PuBe neutron source are somewhat more encouraging. In that case the alcohol resulted in 21 to 26% greater response than that of the dry dosimeters. The higher neutron energy, combined with a less-intense gamma radiation background, provide a more favorable situation for the successful application of this dosimetry system. Additional experiments will be necessary to develop this thermoluminescent system into a workable personnel neutron dosimeter.

HIGH EXPOSURE RATE EXPERIMENTS

A series of experiments at very high exposure rates was conducted using the Health Physics Research Reactor at Oak Ridge National Laboratory. Measurements of fast neutron and gamma radiation ray exposure was made, both in air and behind 8 in. of graphite at a distance of 3 m from the pulsed reactor. The results of these measurements (Table III) were used mainly to calibrate the dry versus wet thermoluminescent dosimeters for these exposure conditions. The gamma radiation exposure measurements by the dry LiF dosimeters were consistent with measurements by silver-activated phosphate glass dosimeters.

TABLE III. High Exposure Rate Experiments

Dosimeter	Fast Neutron Dose (rads)	γ-Ray Exposure (R)	Geometry
		Burst #1	
TLD 1	600	85	On burro @ 3 meters
TLD 2	352	50	In air @ 3 meters
TLD 3	375	49	In air @ 3 meters
TLD 4	395	53	In air @ 3 meters
Fission foils	330	--	In air @ 3 meters
Ag glass	-	58	In air @ 3 meters
		Burst #2	
TLD 5	78	20	Behind 8 in. graphite @ 3 meters
TLD 6	114	20	Behind 8 in. graphite @ 3 meters
TLD 7	82	21	Behind 8 in. graphite @ 3 meters
TLD 8	64	20	Behind 8 in. graphite @ 3 meters
Fission foils	81	--	Behind 8 in. graphite @ 3 meters
Ag glass	--	22	Behind 8 in. graphite @ 3 meters

A neutron sensitivity of 4 reader units per 100 mrads was used to obtain the neutron dose figures shown for burst 1 and burst 2. Gamma and neutron dose measurements on the burro, used to simulate a human, during burst 1 were, of course, considerably higher than measurements in air at the same distance (3 m) due to backscattering. On burst 2, one of the neutron measurements was considerably higher than, one was lower than, and the other two were close to the measurements by fission foils which are considered as the standard dose measurement for these experiments. The reason for the apparently higher sensitivity of the LiF dosimeters to the low dose rates from the PuBe neutron source is not known (4 reader units/100 mrads for burst type exposures compared to 6 reader units/100 mrads for neutron source exposures). It would seem from these measurements that the LiF as a neutron dosimeter is rate dependent. The neutron dose rate for burst 1 was about 6.5×10^6 rads/sec, and for burst 2 was about 1.7×10^6 rads/sec. The neutron dose rate from the neutron sources was a few tens of mrads/hr.

LiF IMBEDDED IN TEFLON

Studies of the characteristics of teflon-LiF plastic discs were started late in the year. These discs are particularly suited for applications in hand dosimeter measurements where they can be used in place of dosimeter film in finger ring dosimeters. These studies were directed with this application as an immediate objective. For the first experiments, the material was used in the form of 1/2 in. diam discs about 0.015 in. thick. Each disc contained about 20 mg of LiF. The discs were exposed, in groups of five, to various exposures of radium-gamma radiation up to a maximum exposure of 10 R. The response to these exposures was nearly linear; deviations from a straight line were less than ±3%. Figure 9 shows the exposure response curve with the data points.

A special planchet with a stainless steel screen is used to hold the teflon-LiF disc in good contact with the heating surface of the planchet for readout. Holes of various sizes were cut in the screen to permit as much light as possible to reach the photomultiplier during readout. Satisfactory readout was obtained with holes as large as 3/8 in. in the screen, though some care needs to be taken to assure that the disc is centered in the hole and pressed down firmly on the planchet surface for good heating.

Background readings of the discs as obtained from the manufacturer averaged about 17 reader units with a 3/8 in. diam hole in the planchet. Exposures to 200 mR radium gamma yielded an average readout of 68 reader units or a difference above background of about 50 units. The discs can accurately measure exposures of 100 mR.

The energy response of the discs was determined by comparing their monoenergetic X-ray response with their response to radium gamma radiation. The results of the measurements shows a peak in sensitivity at about 23 keV and a gradual decrease in sensitivity as the energy increases up to about 100 keV. At the peak,

the response is about 40% higher than at the effective radium gamma radiation energy. These results are shown in Figure 10. For the energy response study, the standard Hanford finger rings were used with a plastic shield 0.016 in. thick in front of the teflon-LiF disc.

THERMOLUMINESCENT READER DEVELOPMENT

P. C. Friend

The design of thermoluminescent readers requires consideration of four major factors: 1) Uniform and consistent detector material heating; 2) thermoluminescent heating chamber design that permits rapid and thorough

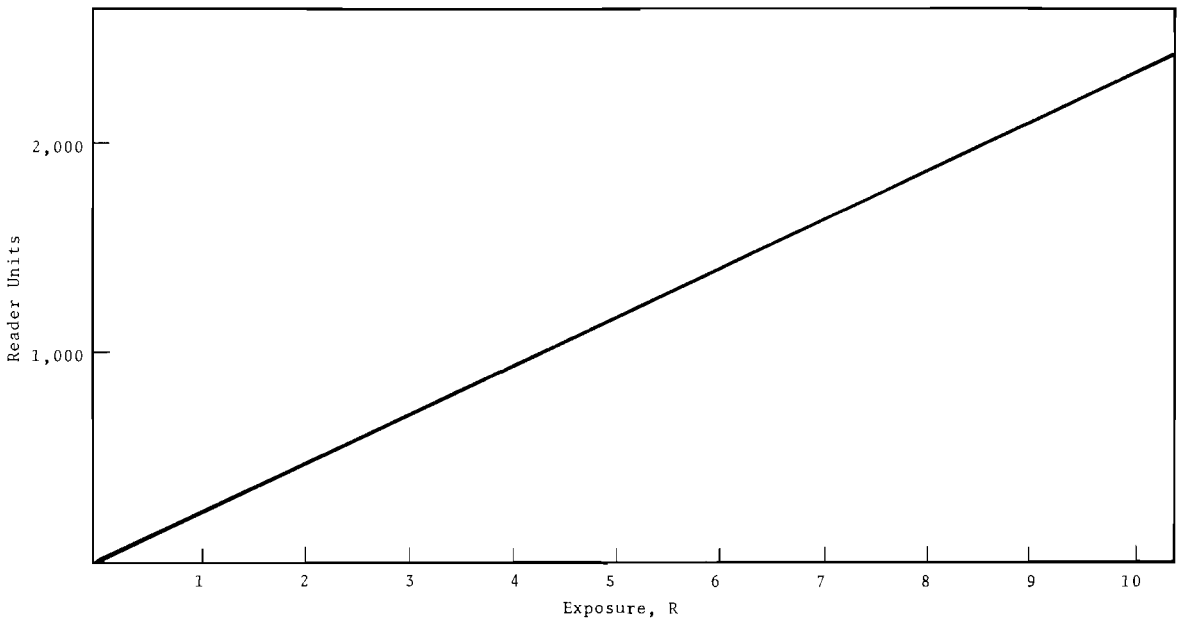

FIGURE 9. Exposure Response of LiF-Teflon Discs (Ra γ Exposures)

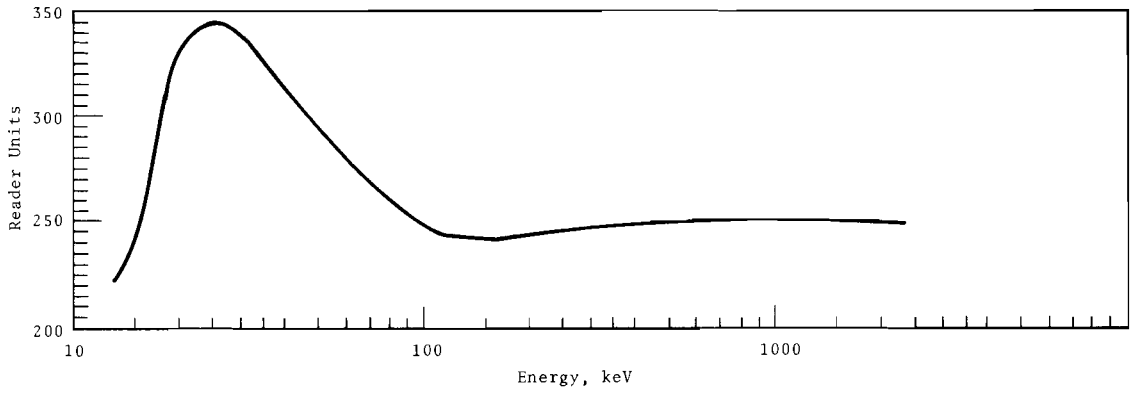

FIGURE 10. Photon Energy Dependence of LiF-Teflon Discs

gas flush with light-tight seals; 3) optical system design which permits measurement of all luminescent light emitted but not black body radiations from the planchet; and 4) a high signal-to-noise ratio in the light measurement system. Commercially available thermoluminescent readers have not fully met the research and development requirements in all of these areas. Research and development to improve the gamma, X-ray, and neutron radiation dose measurements through the use of thermoluminescent material have led to the design, construction, and calibration of a thermoluminescent reader meeting the basic requirements stated above.

An extremely low dark current and high cathode sensitivity was attained from a selected photomultiplier tube. The anode dark current of this tube is equivalent to only 0.15 picolumens. The dark current of the tube used in the commercial reader was 30 picolumens. The dark current and high cathode sensitivity of the selected photomultiplier tube improved the reader signal-to-noise ratio by approximately $(30/0.15)^{1/2}$ or 14. An infrared filter and a special glass light coupler on the photomultiplier tube also increase the signal-to-noise ratio.

An integrating digital voltmeter counter is used as the main analog-to-digital converter and simultaneously performs the integrations of the light scintillations for dose readout and the power to the planchet to assure reproducible dosimeter material heating. The power and the total integrated energy to the planchet holding the thermoluminescent material can be independently controlled. A current up to 200 A can be passed through various experimental planchets requiring up to 3 V of electromotive force. Although the high pressure electrical contacts operated by a two-way air cylinder have a low and reproducible resistance, the electrical energy absorbed in the planchet will be electronically controlled independent of the contact resistance by the voltmeter-counter.

SOLID STATE PARTICLE DETECTORS AND DOSIMETERS

W. V. Baumgartner and L. W. Brackenbush

INTRODUCTION

Many crystalline materials, plastics, and glasses are damaged by the passage of charged particles through the material. If the linear rate of energy transfer in the material is high enough, the materials are damaged so that certain etches will attack the areas where the particles have passed, and etch pits will appear. Particles will produce tracks only if the linear rate of energy transfer is higher than a critical rate of energy transfer which is a property of a specific material. Large doses delivered by particles which do not provide the minimum critical rate of energy transfer as they pass through a material seem to have little or no effect. This property may be used to identify the mass and energy of light particles.

Heavy charged particles such as fission fragments produce damage areas which can be made visible by etching many materials such as mica and almost all plastics which can be etched without disintegrating. (Typical plastics

are bisphenolacetonecarbonate plastic, cellulose nitrate, cellulose acetate, cellulose acetate butyrate, etc.) Light particles such as alpha particles produce tracks only in certain materials such as cellulose nitrate. Experiments using hydrocholoric acid, nitric acid, and concentrated sodium hydroxide solutions as etches showed no tracks in lucite (polymethylmethacrylate), polyethylene, Formvar, (polyformal), and polystyrene because these etches did not attack the plastics or dissolved them rather than etching the surface.

There is usually a variety of etches which can be used to delineate the tracks in a material. For glass, 28% sodium hydroxide solution, hydrofluoride acid, 20% ethylenediaminetetracetic acid (EDTA), etc., act as etches at 60 °C with etching times of a few minutes. Hydrofluoric acid is the best etch for mica with etching times of a few seconds to a few minutes for various types of micas etched at room temperature (20 °C). Most plastics are conveniently etched in 6 N sodium hydroxide solutions at 65 °C for periods of about 30 to 60 min. This etch gives large, well defined tracks which are easily observed under a 200 X microscope. Shorter etch times (e.g., 20 min) give smaller tracks which are easier to count if the track density is quite high. Cellulose nitrate requires etching of only a few seconds in hot 6 N caustic solution for tracks to appear. Both fission fragments and alpha particles damage the cellulose nitrate plastic sufficiently to cause etch pits, although the alpha tracks are much smaller and are difficult to differentiate from small etch pits caused by imperfections in the plastic.

The properties of these particle track detectors make them useful for a wide variety of applications--neutron dosimetry, proton and high energy charged particle dosimetry, plutonium bioassay, detection of trace quantities of fissionable materials, etc.

NEUTRON DOSIMETRY

Foils of various fissionable materials placed next to plastic films can be used as neutron dosimeters by counting the number of fission fragment tracks for a given neutron dose. The general principle of the concept is illustrated in Figure 11. Approximate neutron spectra measurements can be made by using fissionable isotopes which exhibit a definite cutoff below certain neutron energies, Figure 12. For the current experiments, U^{238} is used to measure neutron dose above 1.3 MeV, Np^{237} is used to measure neutron dose above 0.4 MeV, cadmium-covered U^{235} is used to measure neutrons above 0.7 eV, and bare natural uranium is used to measure thermal neutrons. The neptunium is in the form of neptunium oxide surface supported in a slowly cured polyester plastic. This method can measure neutron doses as low as a fraction of a rad. It was used successfully on plutonium fluoride hoods in plutonium production facilities to measure long-term integrated neutron dose when NTA emulsion neutron badges were completely blackened by gamma radiation and therefore impossible to evaluate. The

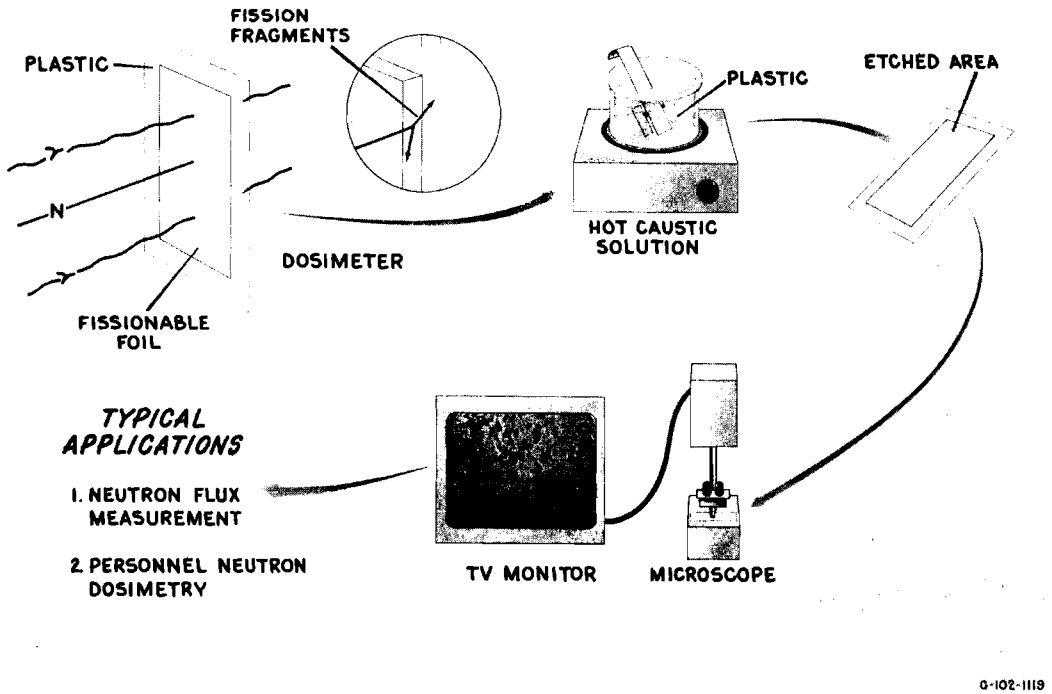

FIGURE 11. Fission Foil Neutron Dosimeter

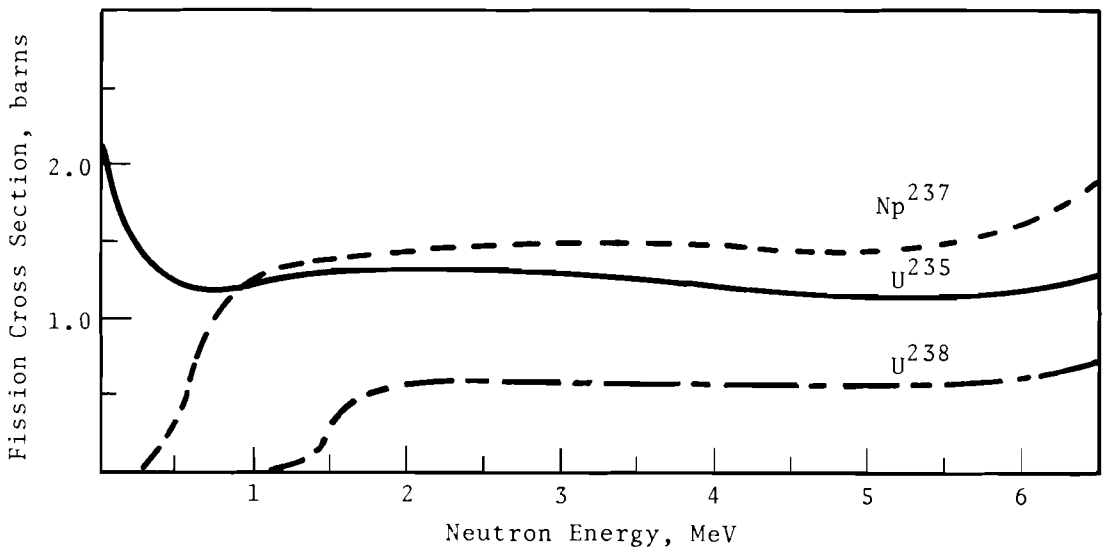

FIGURE 12. Cutoff Energies and Cross-Sections for Various Fissionable Isotopes

minimum detection limit is determined by the area of the fission foil and by the statistical accuracy desired. A detection limit of approximately 10 mrad for fast neutrons and 0.5 mrad for thermal neutrons for each square centimeter of detector used is obtained with the fission foils named above.

Prototype dosimeters were exposed to nearly monoenergetic neutrons produced by a positive ion Van de Graaff

accelerator. The response of the various fission foils is shown in Figure 13. Note that the small amount of U^{235} in the 20-fold depleted uranium does not greatly influence the cutoff point for this fission foil.

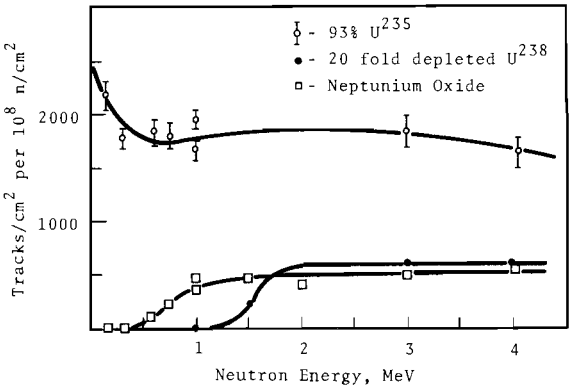

FIGURE 13. Relative Response of Various Fissionable Isotopes

The relative response of the various fission foils to neutrons of various energies is shown in Table IV. Fast neutron data are from a 4.7 MeV neutron exposure on a Van de Graaff accelerator, and thermal neutron data are from exposures in a Sigma pile with neutron sources calibrated by the National Bureau of Standards. All plastic detectors studied have a 100% efficiency in recording fission fragment tracks. Consequently, the values reported in Table IV are valid for all plastic detectors. A study over a 1 yr period indicated that the fission fragment neutron dosimeters were essentially free from track fading.

TABLE IV. Relative Response of Fission Foils

	Fast Neutrons (4.7 MeV)	Thermal Neutrons (Sigma Pile)
U^{238} (20 fold depleted)	1.9×10^5 n/track	
NpO_2 (on plastic base)	2.5×10^5 n/track	
U^{235} (93%)	8.5×10^4 n/track	3.4×10^2 n/track
Cd covered U^{235} (30 mil Cd)	1.1×10^5 n/track	4.7×10^4 n/track
Natural U		3.6×10^4 n/track

Several measurements were made on plutonium fluoride hoods at the plutonium fabrication facility. Neutron film badges containing conventional NTA film were exposed simultaneously; however, the dose was impossible to evaluate with the NTA film due to fogging of the film by gamma rays. Typical results of the plutonium fluoride hood exposures evaluated from fission fragment dosimeters are shown in Table V, for dosimeters exposed in pairs.

TABLE V. Plutonium Fluoride Hood Exposures

Dosimeter Number	Fluence (n/cm^2) Above 1.3 MeV (U^{238})	Fluence (n/cm^2) Above 0.4 MeV (NpO_2)	Dose (rads) Above 1.3 MeV	Dose (rads) 0.4-1.3 MeV	Dose (rads) Total
1	7.0×10^7 n/cm	20×10^7	0.25	0.30	0.55
2	8.5×10^7	22×10^7	0.30	0.31	0.61
3	6.4×10^7	17×10^7	0.22	0.36	0.58
4	6.3×10^7	13×10^7	0.22	0.14	0.36
5	2.3×10^7	3.8×10^7	0.082	0.034	0.12
6	2.2×10^7	3.8×10^7	0.076	0.037	0.11

Fission fragment neutron dosimeters have several distinct advantages over conventional neutron film dosimeters. The neutron film badge dosimeters containing NTA film are not sensitive to neutrons below about 0.8 MeV, while the fission fragment dosimeter can detect neutrons with energies as low as 0.4 MeV. A fission fragment neutron dosimeter with only a neptunium oxide foil can give more accurate information about the neutron dose than NTA emulsions. There are no track fading or gamma fogging problems associated with fission fragment techniques. The fission fragment dosimeters are easier to evaluate for there is no darkroom processing and the tracks are large and easy to count.

ALPHA PARTICLE DETECTION

Cellulose nitrate seems to be the only common plastic which will record alpha particle tracks of a few MeV energy. Commercial cellulose nitrate plastic contains camphor and other plasticizers which cause thousands of small surface defects per square millimeter that cannot be readily be distinguished from alpha particle tracks. A film which is almost free from "background" tracks and imperfections can be prepared from highly purified pyroxylin (Paralodion) dissolved in ethyl acetate or amyl acetate. The material is spread on a clean glass surface, allowed to dry very slowly and then annealed at 400 °F for 15 min.

It is not possible to observe the tracks of four or five MeV alpha particles on the surface of cellulose nitrate because the linear rate of energy transfer is less than the critical rate required for cellulose nitrate damage. As the alpha particles travel through the plastic, the rate of energy transfer increases until near the end of the alpha particles range when the rate of energy transfer suddenly decreases. The alpha tracks can be observed by etching away the surface or by degrading the alpha particles through thin plastic films. An alpha spectrometer using lithium-drifted semiconductors was used to measure the alpha spectrum after particles from very thin plutonium alpha sources were degraded in energy by thin 0.5 mil plastic films. The alpha particles which have energies between about 3.5 and 4.5 MeV have a sufficiently high linear rate of energy transfer to cause track formation in cellulose nitrate. The detection efficiency of alpha particles by cellulose nitrate has not been determined.

DETECTION OF TRACE FISSIONABLE ISOTOPES

It is possible to use fission fragment track detectors for the quantitative measurement of very small amounts of fissionable materials. A technique was developed for detecting trace amounts of plutonium corresponding to 0.01 dis/min (about 10^{-12} g) of plutonium alpha activity. Plastic strips are placed upon electroplated planchettes and exposed to fluences of about 10^{15} thermal neutrons/cm^2 along with a set of standards of known plutonium content. The plastic strips are then etched in a 6 N sodium hydroxide solution at 65 °C for about 1 hr. The number of tracks on the

Lexan plastic are counted under a microscope at about 200 X. The principle is illustrated diagrammatically in Figure 14. The amount of plutonium on the planchettes can be determined from a plot of the number of tracks versus the amount of plutonium on the standards as shown in Figure 15.

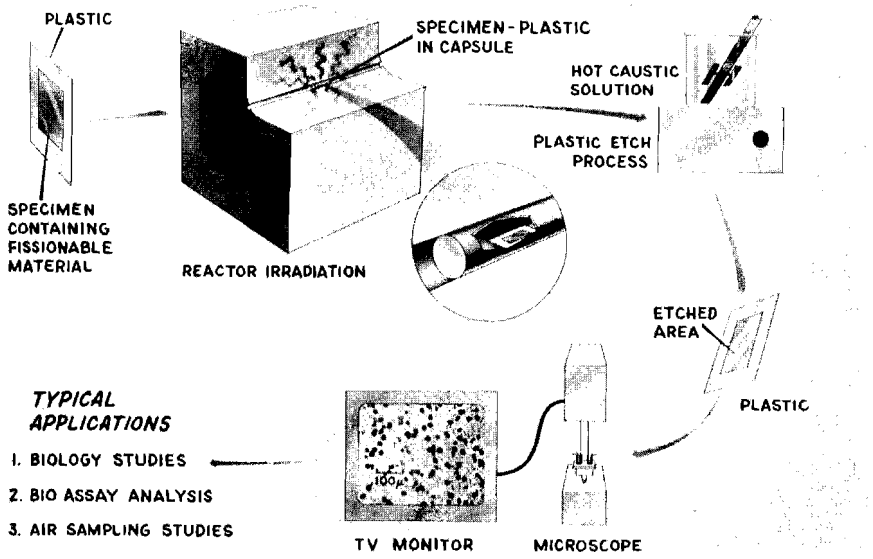

FIGURE 14. Low Level Fissionable Material Detector

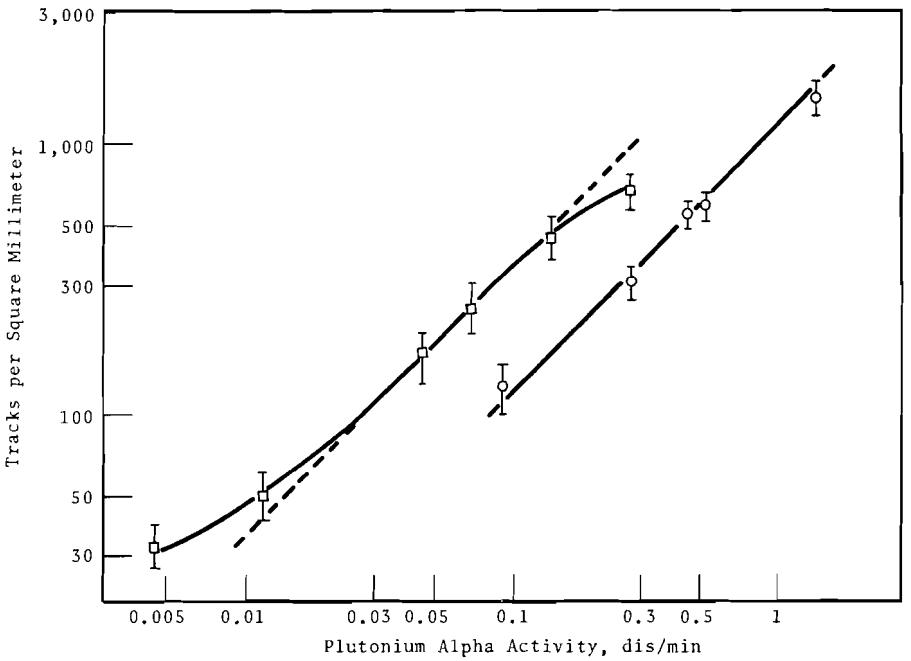

FIGURE 15. Relationship Between Number of Tracks and Plutonium Content for Two Sets of Samples Exposed Between 10^{15} and 10^{16} Neutrons/cm^2

This method has the advantages of being very sensitive, rapid, and reasonably accurate, but requires large fluences of thermal neutrons. It does not have the disadvantages of conventional NTA emulsion techniques--track fading, long exposure times (a week or more) for very low level samples, and the high magnification required to count the alpha tracks in NTA film. It is possible to eliminate the tedious track counting by using a scanning microscope and dark field illumination.

For very low level work (below 0.01 dis/min of plutonium alpha activity), it is necessary to take special precautions to control the amount of background fissionable material. Studies have shown that some activity is retained on the electrodeposition apparatus if used for several sample runs. To lower the detection limit, it is necessary to:

(1) Adopt "white room procedures." A filtered air hood is presently used to eliminate airborne dust containing uranium and seems to be reasonably effective.
(2) Use reagents having very low fissionable material content.
(3) Use thoroughly clean electrodeposition apparatus.
(4) Develop inexpensive molded plastic electrodeposition cells which can be disposed of after each use, or use easily decontaminated cells made of plastics (such as teflon) which are chemically inert and do not crack on the surface.

By using this system of analysis, it was possible to obtain blank samples with traces of fissionable material corresponding to 0.0008 dis/min of plutonium alpha activity.

ACTIVATION TYPE PERSONNEL NEUTRON DOSIMETER

L. F. Kocher

INTRODUCTION

The monitoring of fast neutron dose for personnel dose evaluation by the use of nuclear track film is well established. The deficiencies in the performance of the nuclear track film dosimeter are principally: (1) High dose detection limit, (2) fading of tracks, (3) gamma radiation interference, (4) inadequate energy response, (5) tedious evaluation procedures. Development programs at Battelle-Northwest during the past year have advanced several new concepts which have shown promise as a replacement for the nuclear track film dosimeter.

The new dosimeter described here contains metal activation foils and an ordinary beta gamma film packet. The dosimeter depends upon the moderation and backscatter of fast neutrons by the human body to provide for activation of the dosimeter foils. The path of the typical incident fast neutron is as follows:

(1) Penetration through the dosimeter components into the body.
(2) Moderation within the body tissues.
(3) Backscatter from the body to the neutron dosimeter.

(4) Capture by an activation foil in the dosimeter.

Decay of the activated foil then darkens the film packet providing a record of the neutron dose. A delicate balance among the incoming neutron energies, the fraction of the neutrons absorbed or backscattered by the body, and the absorption cross-section of the activation foil for each energy encountered must be satisfied if the film darkening is to bear an interpretable relationship with the delivered dose. A developmental program to provide dosimeter components and dosimeter geometries suitable for use over a full energy spectrum of neutrons is now in progress.

DOSIMETER DESCRIPTION

The dosimeter contains three metal filter areas: namely, tin-rhodium, cadmium-rhodium, and tin-iron (Figure 16). These combinations of filters were chosen by calculation and experimentation to give the desired dosimeter response. The density behind the tin-rhodium filter is produced by gamma radiation, thermal neutron radiation, and "body moderated" fast neutrons. The density behind the cadmium-rhodium filter is produced by gamma radiation and "body moderated" fast neutrons. The density behind the tin-iron filter is produced by photon radiation. The filter thicknesses are chosen so that the photon produced density behind each filter is identical for any given exposure over the energy range from about 0.020 MeV to 3 MeV.

With this filter system, three different density measurements for three qualities of radiation--namely; photon, thermal neutron, and intermediate to fast neutron--are obtained. A set of simultaneous equations can

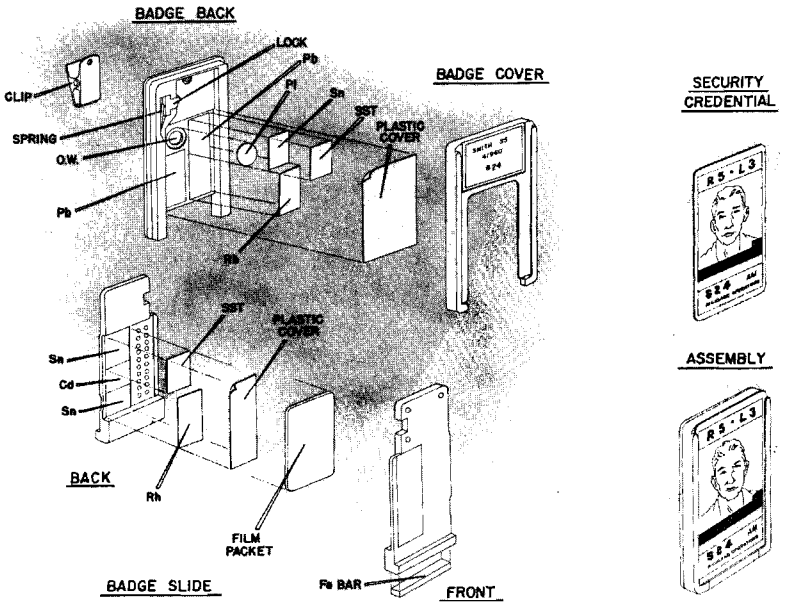

FIGURE 16. Activation Neutron Dosimeter

be established to permit the calculation of the dose contributed by each radiation component.

In general, for a radiation field consisting of beta particles, photons, thermal neutrons, and intermediate and fast neutrons, the following set of equations define the film density for each filter region:

$$D_{BA} + D_{\gamma A} + D_{n_f A} + D_{n_t A} = D_A \quad (1)$$

$$D_{BB} + D_{\gamma B} + D_{n_f B} + D_{n_t B} = D_B \quad (2)$$

$$D_{B_C} + D_{\gamma C} + D_{n_f C} + D_{n_t C} = D_C \quad (3)$$

where

D_{BA} = Density behind filter A due to beta radiation

$D_{\gamma A}$ = Density behind filter A due to photon radiation

$D_{n_f A}$ = Density behind filter A due to intermediate and fast neutron radiation

$D_{n_t A}$ = Density behind filter A due to thermal neutron radiation

D_A = Total density behind filter A

The symbols in Equations 2 and 3 are similiarly defined for filters B and C, respectively.

The filter system is designed so that conditions described in Equations 4 through 9 are met. The filters are sufficient in density thickness (mg/cm^2) to yield essentially zero film density behind all three filters for beta particles of energies <3 MeV.

$$D_{BA} = 0 \quad (4)$$

$$D_{BB} = 0 \quad (5)$$

$$D_{BC} = 0 \quad (6)$$

The density thickness of all three filters was chosen to provide equal film densities when the system was exposed to photon radiation.

$$D_{\gamma A} = D_{\gamma B} = D_{\gamma C} \quad (7)$$

Filters B and C were chosen to provide equal film densities when exposed to fast neutron radiation.

$$D_{n_f B} = D_{n_f C} \quad (8)$$

All filters were chosen to provide unequal response from thermal neutron radiation

$$D_{n_t A} \neq D_{n_t B} \neq D_{n_t C} \quad (9)$$

Applying conditions of Equations (5), (6), and (7) and subtracting Equations (2) and (3),

$$(D_{n_t C} - D_{n_t B}) = D_C - D_B \quad (10)$$

Subtracting Equations (1) and (2), and spplying the conditions of Equations (4), (5), and (7),

$$(D_{n_f B} - D_{n_f A}) = D_B - D_A - (D_{n_t B} - D_{n_t A}) \quad (11)$$

The absolute value of the terms in parenthesis in Equations (10) and (11) need not be determined. The difference between the terms is sufficient to define the dose values

desired from this dosimetry system. For absolute accuracy in the use of Equations (10) and (11), calibrations should be performed with intermediate and fast neutrons and thermal neutron radiations similar in energy spectrums to those to be measured.

INTERPRETATION

To interpret a neutron film dosimeter that was exposed to beta, photons, intermediate and fast neutrons, and thermal neutron radiations, the density behind each of the three filter areas is measured. The dose interpretation for thermal neutrons and intermediate and fast neutrons is made as follows:

Neutron Radiation from Thermal Neutrons

The density behind Sn-Rh filter (D_C) and the Cd-Rh filter (D_B) areas results from photon radiation, thermal neutron radiation, and fast neutron radiation. The response characteristics of the filter system are chosen so that the photon radiation and fast neutron radiation produces equal densities behind each of these two filters. For slow neutron radiation, the Cd-Rh filter absorbs most of the slow neutrons; consequently, the difference in density behind the Sn-Rh and Cd-Rh filters ($D_C - D_B$) can be directly related to the thermal neutron dose equivalent by use of a calibration curve, Figure 17 is a typical calibration curve for thermal neutrons.

Neutron Radiation from Intermediate And Fast Neutrons

The density behind Cd-Rh (D_B) and the Sn-Fe filter (D_A) areas results from intermediate and fast neutrons, thermal neutrons, and photons respectively. The difference in density between these two filters ($D_B - D_A$) is a function of fast and thermal neutron radiation, Equation (11). Since the thermal neutron dose equivalent is independently determined from the Sn-Rh and the Cd-Rh filter density difference, it is possible to correct the density difference observed between the Cd-Rh and the Sn-Fe filter area for the thermal neutron dose equivalent contributions by an appropriate calibration correction curve. After this correction is made, the remaining density difference between the Cd-Rh and Sn-Fe filter may be related to a fast neutron calibration curve; and the fast neutron dose equivalent is determined. Figure 18 is a typical fast neutron calibration curve for neutrons from a PuF_4 neutron source.

The experimentally observed neutron energy response, when calibrated on a human phanton, differs by a factor of about 100 for neutron energies of 0.020 MeV and 5 MeV, Figure 19. This energy dependency is, of course, far beyond that which can be tolerated for regular personnel dosimetry applications in a full neutron energy spectrum. Special purpose applications, where the neutron spectra are known, may permit energy corrections to be made; and satisfactory neutron dose measurements can be obtained. For applications

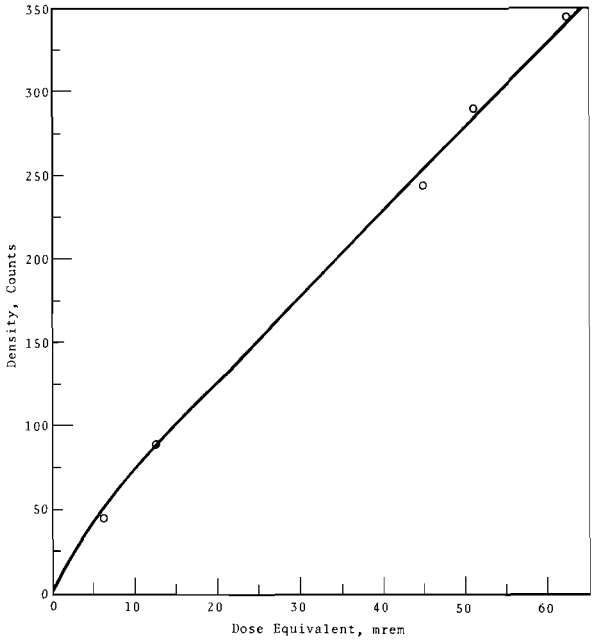

FIGURE 17. Thermal Neutrons Dose Equivalent Versus Density

where the neutron spectrum range is limited to a few MeV, the dosimeter can be satisfactorily used. For example, for the neutron energy range from 1 MeV to 5 MeV, the response per unit dose varies by a factor of about 4. When neutron sources such as PuBe are the only source of neutrons, the energy response characteristics may be accounted for in the dosimeter calibration and satisfactory neutron dose equivalent measurements are obtained. Studies on the design of a shield system with a more appropriate energy response are being considered.

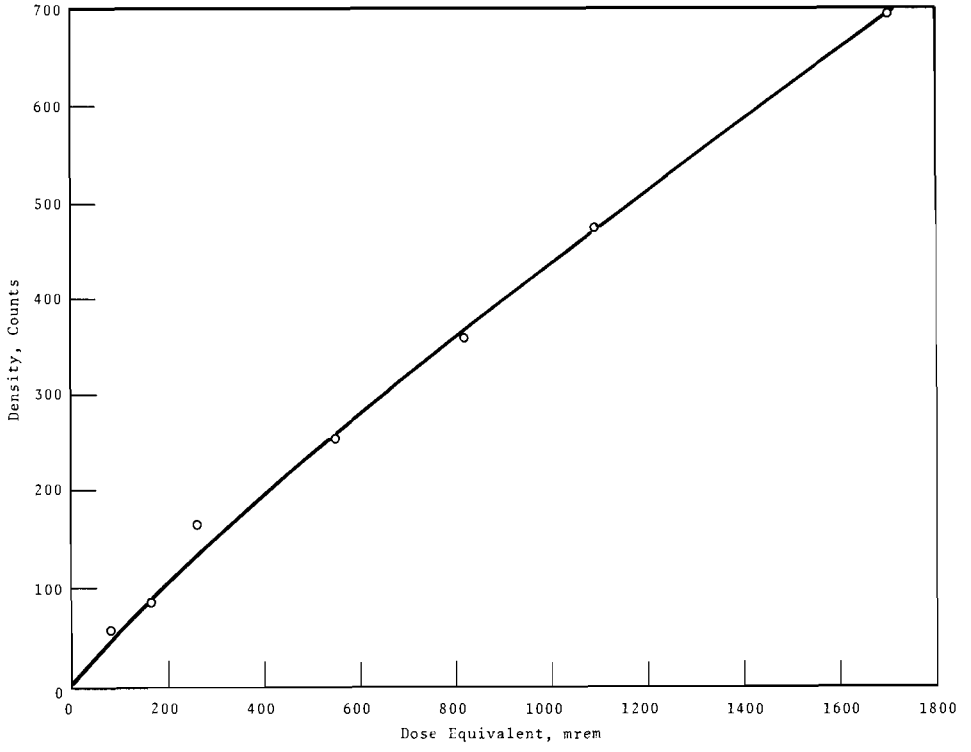

FIGURE 18. Fast Neutron Dose Equivalent Versus Density PuF_4 Source

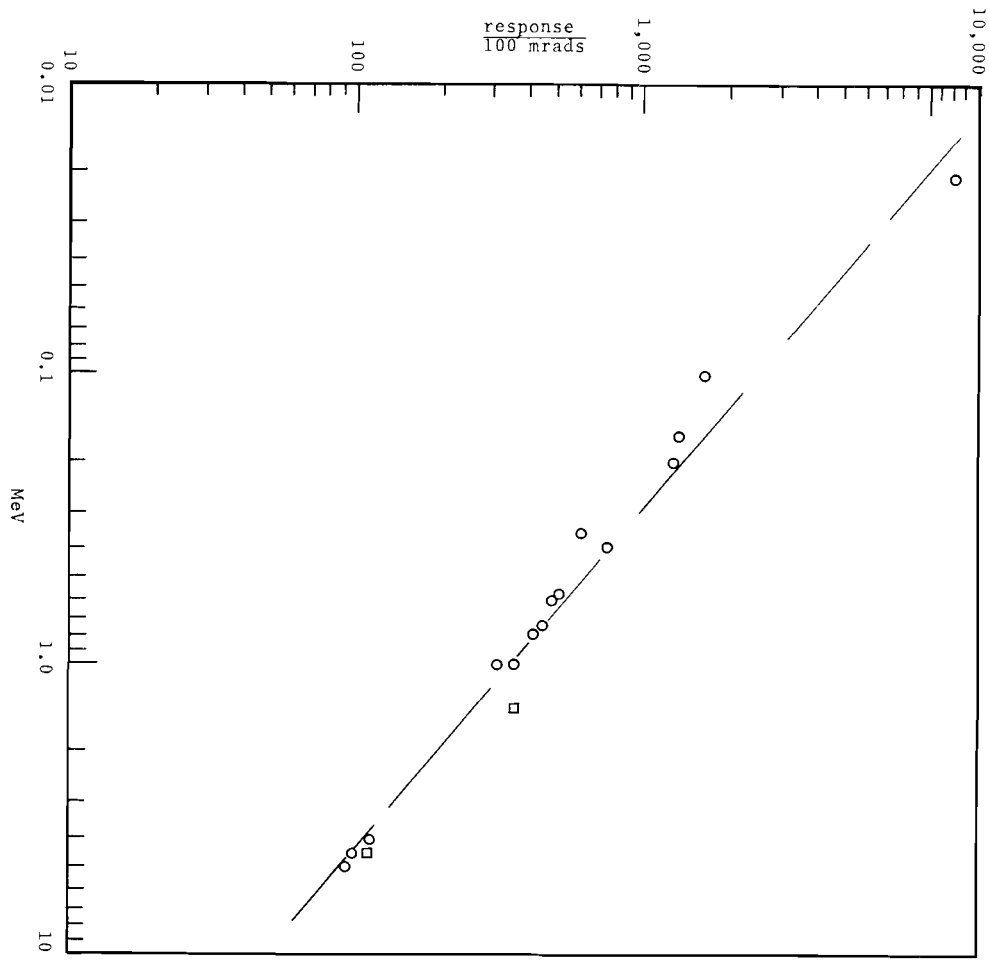

FIGURE 19. Activation Neutron Dosimeter Energy Response

PORTABLE FILM DENSITOMETER

P. C. Friend and L. F. Kocher

A simple and stable film densitometer circuit was developed and three basic readout methods used in three applications of the circuit. Figure 20 shows the simple external controls and reading station of the film densitometer.

The simplest readout method, manual null balance, consists of a ten-turn potentiometer with dial and a sensitive meter for null indication. This was incorporated into a portable densitometer for film density studies.

The second type of readout uses a commercially available servo-balanced potentiometer with a digital turns counter automatically presenting the reading. This unit, smaller than a portable typewriter, provides an automatic visible readout linear with exposure for the Hanford film badge dosimeter over the exposure range from zero to about 2 R of radium-gamma radiation.

The third type of readout was used to modernize an old scanning microdensitometer. Again, a commercially available servo-driven null balance potentiometer was used; but, instead of the turns-counter providing a

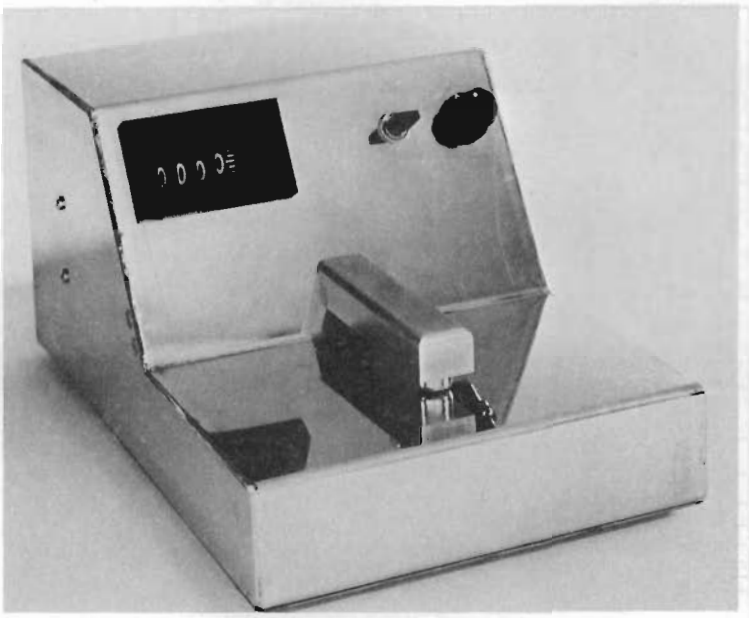

FIGURE 20. Portable Film Densitometer

digital readout, a pen was driven by the servo-motor to permit an analog recording. In this application of the basic densitometry circuit, all of the DC amplifier, power supplies, and drift problems were discarded and replaced with a simpler and more stable circuit. The existing 18 A, 5 V lamp and optical system were replaced with a new lamp and optical system requiring only 1% as much power to provide about the same intensity of well-regulated light. The same type of efficient lamp was used in the other two densitometers.

GAMMA RADIATION EXPOSURE RATES MEASUREMENTS

W. V. Baumgartner

The measurement of radiation exposure rates in 7 MeV gamma radiation fields results in the need for special calibrations of the detection instruments and radiation dosimeters. Instrumentation designed to measure exposure rates to 1 R/hr in these fields was studied. The equipment was calibrated at gamma energies to 7 MeV by using the 3 MeV Dynamitron at the Boeing Company Radiation Effects Laboratory in Seattle, Washington. A thick calcium fluoride target was used with 1.4 MeV protons to obtain the 7 MeV gamma radiation.

Film badge dosimeter calibration results indicate that, at exposures of about 400 mR, an overestimation of about 40% in the dose received could occur. The increased film darkening at these high energies results from pair production in the tantalum shield area of the Hanford film badge dosimeter. The basic calibration normally provided at radium-gamma or Co^{60}

radiation energies produces film darkening primarily through Compton scattering.

SMALL CHAMBER EXPOSURE RATE INSTRUMENT

F. L. Rising

The Victoreen 440 low energy survey meters were modified by removing the original ion chamber. A probe about 9 in. long with 1 1/2 in. diam by 3/4 in. deep chamber at the end was installed in place of the original ionization chamber. The walls are 1/8 in. thick phenolic, and the front window is 7 mg/cm^2 cellulose acetate. The collecting electrode is a cellulose acetate disc. The chamber parts are graphite coated. The energy response is the same as that of a standard phenolic chamber Cutie Pie instrument. The signal is conducted from the chamber to the instrument by a coaxial cable. The instrument did not possess excessive extracameral effects. A beta rejection shield of 1/8 in. phenolic plastic is used.

The instrument was studied to determine its geometrical response and was found to be substantially superior to the standard Cutie Pie. Measurements of uranium slab surface exposure rates were made with an extrapolation chamber and compared with measurements made with this small chamber instrument. The differences in readings were within the reading errors of the instrument for sources greater than 2 in. in diameter. The range of this instrument is the same as the standard Cutie Pie; three scales--0 to 50 mR, 0 to 500 mR, 0 to 5000 mR.

CRITICAL INCIDENT ALARMS

P. C. Friend

Commonly used critical incident alarms are sensitive to gamma radiation only. For criticality events the large neutron fluences resulting from the event may be utilized to trip alarms with several important advantages over gamma radiation sensitive alarms. Based on this fact, a criticality event detection and alarm system sensitive only to neutron radiations was developed, calibrated and placed into service. This system permits placing the detector units near all potential criticality locations but avoids false alarms due to fluctuating photon radiation levels encountered in day-to-day operations.

A moderated BF_3 tube was selected for use as the detector. These tubes have proven to be reliable, sensitive to neutrons, and insensitive to even 50 R/hr of radium gamma. An all-solid state nonjamming, self-checking circuit with an adjustable trip point was developed and tested. Special long life BF_3 tubes were constructed.

The detection and alarming instrument components of the system are designed with two alarm trip circuits: 1) An adjustable neutron dose rate alarm trip which is commonly set between 0.5 to 1.0 mrads/hr, and 2) An accumulated neutron dose alarm trip of 0.1 to 0.2 mrads provided the dose is delivered in a time period of a few seconds. The alarm horn used is a piercing klaxon howler. The electronics are fast response solid state with built-in redundancy to minimize false alarms due to component or circuit failures. The circuit

design and instrument housing tend to eliminate false alarms produced by power line transits and radio-frequency signals. Unique to this system is the self-auditing feature which automatically signals, at a central control panel, malfunctions of the instrument including failures of the detector and electronic circuits.

Three prototypes were constructed and their performance evaluated at the Oak Ridge National Laboratory's Health Physics Reactor Facility. Three of the presently-used gamma sensitive criticality alarms were simultaneously exposed.

The neutron sensitive alarm units detected the burst of the bare unshielded reactor (about 6×10^{16} fissions) in the following locations:

(1) 20 ft (line of sight) from the reactor core
(2) 400 ft from the reactor on the far side of a hill shielded by 3 ft of concrete
(3) 800 ft from reactor on the far side of the hill shielded by 1 ft of concrete.

The gamma radiation sensitive alarm units did not detect bursts at the non-line-of-sight locations, locations 2 and 3.

Four criticality alarm units were tested at the Sandia Pulsed Reactor Facility at Albuquerque, New Mexico. The units within a radius of 1150 ft of the reactor detected the smallest burst they have ever succeeded in generating, 1.27×10^{15} fissions. Larger bursts were detected as far away as 1900 ft. The reactor was shielded with the following: 1 in. of polyethylene, 1 in. of boron, 7 in. of gypsum, and 54 in. of concrete.

PLUTONIUM DOSIMETRY STUDIES

L. G. Faust

INTRODUCTION

The isotopic composition of reactor-produced plutonium is dependent on several parameters, such as: 1) neutron energy spectrum, 2) neutron flux level, and 3) integrated neutron flux. Some of these parameters, such as the neutron energy spectrum, are functions of the physical properties of the individual reactor and its fuel; and, therefore, the isotopic composition of the plutonium usually varies from reactor to reactor.

The radiation dose rates for plutonium are a function of the isotopic composition of the plutonium. Relationships to relate isotopic composition and gamma and neutron dose rates were developed.

SURFACE DOSE RATES

W. C. Roesch derived an expression for the surface dose rate from plutonium. His expression is given below in Equation 1.

$$Ds = B[F\, h\nu(\mu en/\rho)_T + F_F h\nu_F(\mu en/\rho)_{FT}] \quad (1)$$

where Ds = gamma and X-ray surface dose rate
F = unscattered gamma flux at the boundary
$h\nu$ = photon energy
$(\mu en/\rho)_T$ = mass energy absorption coefficient at each energy $h\nu$ in tissue
F_F = fluorescent X-ray flux at the boundary
B = backscatter correction.

Equation 1 was evaluated for several different energy spectra and plutonium compositions by various individuals.

The most recent evaluation based on the best available energy spectra is given by Equation 2.

$$Ds = 960\ f_{238} + 0.98\ f_{239} + 4.7\ f_{240} + [0.19\ t + 17(1-e^{-0.102\ t})]\ f_{241} + 0.29\ f_{242} \quad (2)$$

where Ds = the surface dose rate in rads/hr

fi = weight fraction of the indicated isotope of plutonium

t = time since chemical separation in days.

Equation 2 includes the slight contribution to the total dose rate from fission products and prompt fission gamma rays caused by spontaneous fission. The terms inside the brackets are the contributions to the total dose rate from Am^{241} and U^{237} respectively. Since these two terms are dependent on time since separation, it is beneficial to process the plutonium as soon as possible after separation. Equation 2 was never previously verified by experiment primarily because of the lack of the process history and accurate isotopic analysis of the plutonium.

The surface dose rate of a plutonium metal sample, 2 in. x 4 in. x 0.100 in. thick, was measured using an extrapolation chamber and a static dry box. The sample was separated on or about July 15, 1964, and the measurements were made October 20, 1964. The isotopic analysis was Pu^{239}, 90.45%; Pu^{240}, 8.58%; Pu^{241}, 0.92%; and Pu^{242}, 0.05%. The measured surface dose rate was 1.7 rad/hr after correcting for the 0.012 in. thick plastic bagging material. The original 0.012 in. thick plastic attenuated the true surface dose rate by a factor of 1.3 (23.1%). The calculated surface dose rate for the same material with "t" equal to 97 days is 1.62 rad/hr, a difference of about 5% from the measured value. It is unfortunate that the surface dose rate as a function of time since separation could not be studied to verify that part of Equation 2.

DOSE RATE OF PLUTONIUM METAL AND PuO_2

Experience at the Battelle-Northwest Plutonium Fuels Laboratory indicated that the dose rates present around the process areas were generally larger whenever PuO_2 was present than when just the plutonium metal was present. At first thought, this would seem difficult to explain; however, when one considers the geometries and photon energies involved, the reasons become clear. Because of the relatively low photon energies, the dose rates observed are more nearly proportional to the surface area of the source than to the mass of material present. The presence of PuO_2 or other forms of plutonium powders lead to larger surface areas and, hence, larger observed dose rates even though equal masses of plutonium may be present. Some small additional quantities of ionizing radiations may be produced by the (α,n) reactions in the plutonium compounds but are not important contributors to the dose rate.

To verify our theories, the surface dose rate of the same sample of plutonium--first as metal and then as

PuO_2--was measured. This method eliminated any discrepancy that would be caused by differences in isotopic composition or time since chemical separation. The oxidized plutonium metal was packaged in a cardboard container 2 in. x 4 in. x 0.75 in. thick, thus keeping the mass and exposed surface area of plutonium constant. The surface dose rate was then measured; and, after correcting for the attenuation of the plastic bagging material, a value of 1.6 rads/hr was obtained. This is not significantly different from the value found for the metal (1.7 rads/hr).

For equal exposed surface areas of metal and oxide, nearly equal dose rates are measured. Conversely, a hood containing a quantity of dispersed powdered plutonium will generally produce a higher working dose rate than one containing the same quantity of plutonium as metal blocks.

DOSE RATE OF PuO_2–UO_2 MIXTURES

At the same time that the plutonium metal sample described above was obtained, several samples of PuO_2–UO_2 mixtures were prepared for surface dose rate measurements. In some of the samples, the isotopic composition of the plutonium was held constant and the weight percent of PuO_2 was varied; in others the weight percent of PuO_2 was held constant and the isotopic composition was varied. Table VI summarizes the measured dose rates.

The data in Table VI was used to derive a mathematical expression for the surface dose rate. A graph of these dose rates is given in Figure 21 and the best fit equation of the curve was found using a least squares fit

TABLE VI. Measured Surface Dose Rates

Material	Composition	Plutonium (wt%)	Dose Rate (rad/hr)
PuO_2–UO_2	^{239}Pu - Unknown	1	0.24
PuO_2–UO_2	^{240}Pu - 8%	3	0.30
PuO_2–UO_2	^{241}Pu - Unknown	5	0.37
PuO_2–UO_2	^{239}Pu - Unknown ^{240}Pu - 2.2% ^{241}Pu - Unknown	3	0.24
PuO_2–UO_2	^{239}Pu - Unknown ^{240}Pu - 8% ^{241}Pu - Unknown	3	0.30
PuO_2–UO_2	^{239}Pu - Unknown ^{240}Pu - 16.5% ^{241}Pu - Unknown	3	0.37
PuO_2–UO_2	^{239}Pu - Unknown ^{240}Pu - 27.3% ^{241}Pu - Unknown	3	0.47
PuO_2*	^{239}Pu - 90.451 ^{240}Pu - 8.578 ^{241}Pu - 0.923 ^{242}Pu - 0.048	100	1.57
Pu*	^{239}Pu - 90.451 ^{240}Pu - 8.578 ^{241}Pu - 0.923 ^{242}Pu - 0.048	100	1.69

Both the PuO_2 and Pu were separated about July 15, 2964.

computer program. Equation 3 represents the best fit curve obtained.

$$Ds = 0.2(1-X)^{0.75} + 1.6\ X^{0.75} \quad (3)$$

where

Ds = surface dose rate in rads/hr

X = weight fraction of PuO_2 in the mixture.

Equation 3 will only yield accurate values of the surface dose rate of PuO_2–UO_2 ranges:

Pu^{239}, 90% to 92%; Pu^{240}, 7% to 9%; Pu^{241}, 0.5% to 1%.

NEUTRON DOSE EQUIVALENT RATES

A mathematical expression for the neutron dose equivalent rates resulting primarily from the spontaneous fission of Pu^{238}, Pu^{240}, and Pu^{242}

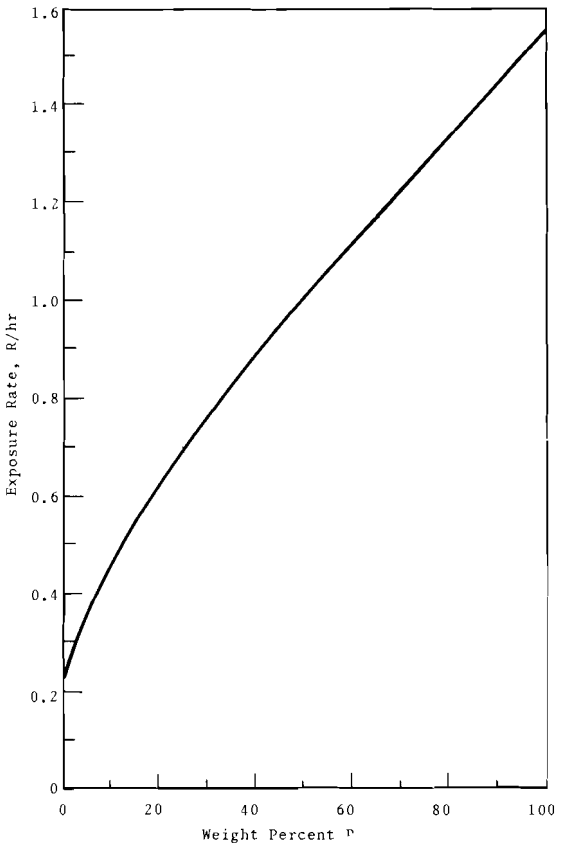

FIGURE 21. Surface Exposure Rate of PuO_2-UO_2 Mixture

was first discussed by W. C. Roesch. The expression he derived for the neutron dose equivalent rate at the surface of a sphere is given in Equation 4.

$$D_{ns} = \frac{2.5 \times 10^{-4}\ n\ M^{1/3}}{\rho} \qquad (4)$$

where

D_{ns} = neutron surface dose equivalent rate in rem/hr

n/ρ = neutrons emitted per gram per second

M = mass of plutonium in grams.

The constant 2.5×10^{-4} is derived from a calculated dose equivalent rate from ^{235}U fission spectrum neutrons of 1.15×10^{-4} rem/hr per neutron/cm^2-sec. Recalculating the constant using seven neutron energy groups yields a value of 8.2×10^{-5} rem/hr per neutron/cm^2-sec. Incorporating this value into Equation 4,

$$D_{ns} = \frac{1.8 \times 10^{-4}\ n\ M^{1/3}}{\rho} \qquad (5)$$

where the terms are the same as in Equation 4. Substituting neutron yield data into Equation 5, and weighting each isotope by its weight fraction gives the following equation:

$$D_{ns} = (0.62\ {}_{238}f + 5.5 \times 10^{-5}\ {}_{239}f + 0.19\ {}_{240}f + 0.31\ {}_{242}f)M^{1/3} \qquad (6)$$

If there are many grams of plutonium present, neutron multiplication takes place; and Equation 6 should be modified by an applicable multiplication constant. Typical values of this constant range from 1 to 1.7 and average about 1.5. The validity of Equation 6 has not been established in the laboratory; however, it was used with excellent results to calculate neutron dose equivalent rates within plutonium fabrication facilities.

TOTAL SURFACE DOSE EQUIVALENT RATES

Whole body exposures to personnel employed in plutonium processing facilities are primarily limited to those caused by ionizing radiations from plutonium itself with the exception of a few storage areas. When the plutonium is primarily composed of the Pu^{239} isotope, the spontaneous fission activity is relatively small; however, with the introduction of high exposure material, e.g., 2,000 MWd/ton or more, the composition of the plutonium is such that the spontaneous fission activity and its resultant

neutron dose equivalent rate will contribute a significant amount to the total whole body exposure. Furthermore, most plutonium process facilities do have some X-ray and gamma ray shielding, usually lead or lead glass in place, which reduced the ionizing radiations without significantly reducing the neutron dose equivalent rate. Table VII illustrates the significance of this effect as well as the dependency of composition on reactor flux. The ratio of X-ray and gamma ray dose equivalent rate to neutron dose equivalent rate varies from 21 to 1 without shielding. The addition of 1/4 in. of lead glass reverses this ratio, e.g., Dg/Dn <1.

CONCLUSIONS

The exposure rate of ionizing radiations from plutonium are a function of the isotopic composition and the time since chemical separation. The neutron dose equivalent rate is a function of mass and isotopic composition. The surface exposure rate equations are valid and can be beneficial to providing estimates of potential exposure rates throughout a plutonium production facility. If shielding for ionizing radiation is employed, it is imperative that neutron dose equivalent rates be established since in all probability the neutron dose equivalent rate will exceed the ionizing radiation dose equivalent rate. This situation will become more predominant as more plutonium from power reactor fuels becomes available for processing.

TABLE VII. Resultant Isotopic Composition and Dose Equivalent Rate from Two Different Fluxes and Same Reactor Residence Time

	$\phi = 5 \times 10^{13}$ Composition w/o Pu								$\phi = 2 \times 10^{14}$ Composition w/o Pu							
T_D*	238	239	240	241	242	Dg**	Dn***	Dg/Dn	238	239	240	241	242	Dg	Dn	Dg/Dn
11.6	0	98.1	1.8	0.1	0	1.07	0.05	21	0	92.1	7.5	0.4	0	1.33	0.21	6.3
23.2		96.1	3.8	0.1		1.14	0.11	10.6		83.9	14.6	1.5		1.79	0.41	4.4
46.3		92.1	7.5	0.4		1.33	0.21	6.3		67.7	27	5.3		2.92	0.76	3.8
81.1		85.9	12.8	1.2	0.1	1.67	0.36	4.6		46.8	40.6	12.6		4.71	1.14	4.1
116		79.6	17.9	2.4	0.2	2.06	0.51	4.0		28.9	45.1	17.6	8.4	5.70	1.66	3.4
232		59.4	31.8	7.5	1.3	3.48	0.95	3.6	0.1	5.1	37	19.9	37.9	6.56	2.82	2.3
463	0.6	29	45.2	17.4	8.4	6.25	1.67	3.7	0.3	0.2	7.9	4.7	86.9	4.38	4.31	1

* *Reactor Residence Time, Days*

** *Gamma and X-ray Surface Dose Equivalent Rates, rem/hr*

*** *Neutron Surface Dose Equivalent Rates, rem/hr*

8.2×10^{-5} rem/hr per neutron/cm^2-sec

ϕ = neutrons/cm^2/sec

MONITORING THE DOSE RATE TO THE G.I. TRACT

P. E. Bramson

INTRODUCTION

A system for continuously monitoring the radioactivity in drinking water, with respect to gastrointestinal (G.I.) tract dose, was developed and placed into routine operation to supplement Hanford's long standing program of radiochemical analyses of

routine grab samples. The grab samples tend to be inadequate particularly because of changes in river flow rate, and intermittent operation of municipal water plants. Radiochemical analyses for individual radionuclide and subsequent calculation of the G.I. tract dose is expensive and time consuming. After consideration of a number of possible monitor configurations, a detector design which simulates the G.I. tract was developed and proved suitable for direct dose rate calibration in the presence of a wide variety of radionuclides in water. A pictorial diagram of this monitoring system is shown in Figure 22.

DETECTOR SYSTEM

The detector consists of a cylindrical Ne^{102} bioplastic well scintillator, 6 in. long with a 2 1/2 in. OD

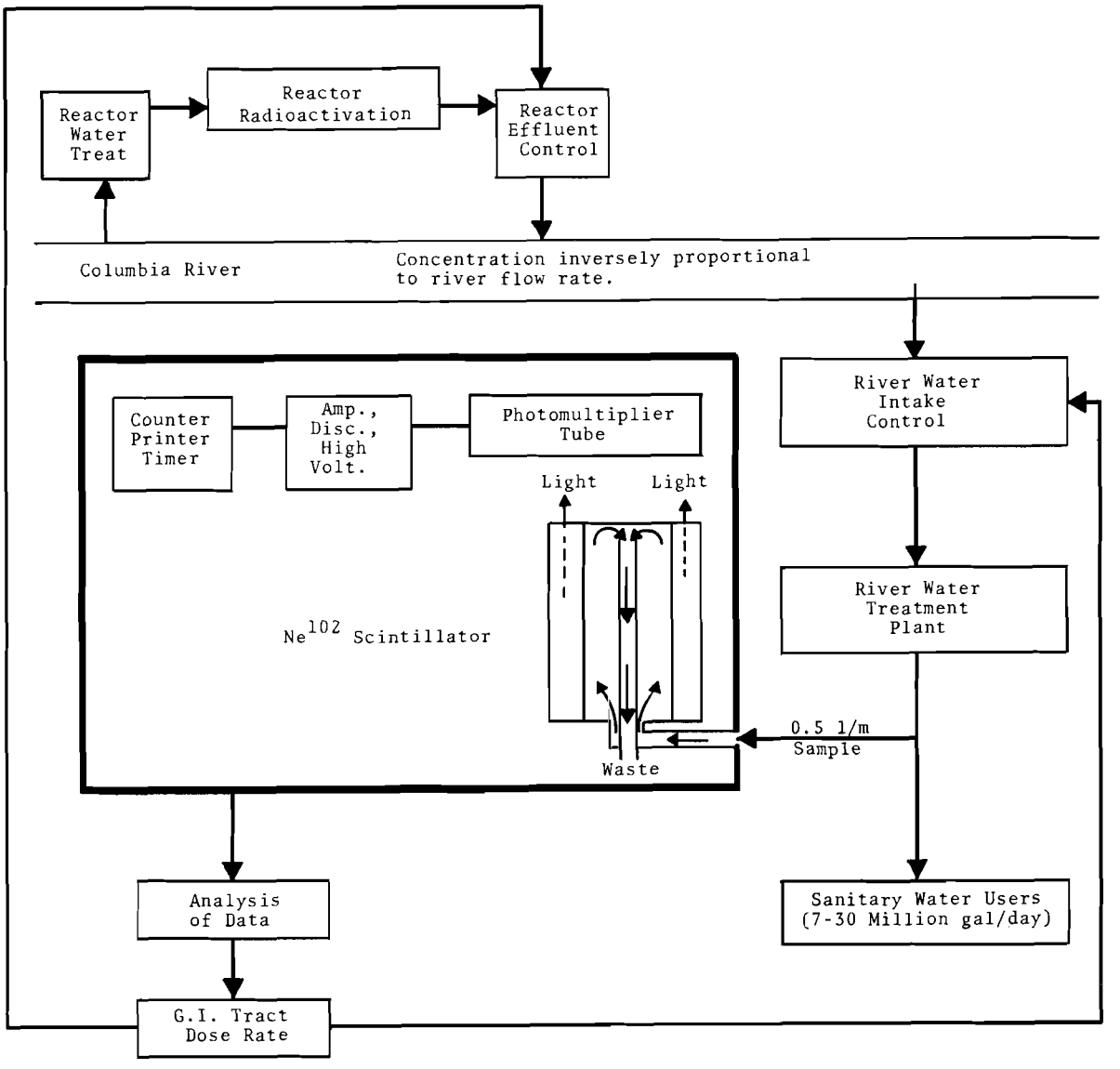

FIGURE 22. G.I. Tract Dose Rate Monitor for Sanitary Water

and a 1/4 in. wall thickness. One end of the scintillator is cemented to a lucite light pipe which couples the scintillator and a 3 in. photomultiplier tube. The inner surface of the well scintillator is covered with a thin, opaque coating of epoxy plastic. This protects the cemented scintillator-lucite joint from damage by moisture and corrosive agents and reduces the possibility of reflection of light into the photomultiplier by the water circulating through the scintillator cavity.

The other end of the cylindrical scintillator is threaded for connection to a copper manifold which admits the water flow to the cavity at the bottom end and extracts the sample at the top through a 1/4 in. copper overflow tube. A continuous water flow through the scintillator cavity is thus maintained. A 1 1/2 in. diam by 5 3/4 in. long polyethylene plug is centered within the scintillator cavity to reduce the water shielding effect on radiation energy dependency while retaining a large sensitive scintillator surface area. Net water space volume of the scintillator is about 135 ml. Two inches of lead shielding is provided on all sides of the detector assembly to reduce background response to a minimum.

Sanitary water system pressure is used to move the continuous water sampling through the scintillator cavity at a rate of about 1 liter/min. One milliliter per minute of distilled water containing 3% NaEDTA by weight is added to the sample flow by a fluid metering pump. Experience has shown that the NaEDTA solution effectively controls radionuclide buildup within the scintillator cavity.

Once every 12 hr, solenoid valves are energized to turn off the sanitary water flow and turn on distilled water flow to flush out the scintillator cavity. The detector count rate is recorded during this flush, giving a measure of background at that time. After 30 min, the solenoid valves are de-energized and the sanitary water flow is resumed.

PERFORMANCE CHARACTERISTICS

Primary contributors to G.I. tract dose from sanitary water derived from the Columbia River are ^{76}As, ^{51}Cr, ^{64}Cu, ^{239}Np, and ^{65}Zn. Ninety percent of the G.I. tract dose rate from consumption of processed Columbia River water results from the decay of these radionuclides.

Each of the aforementioned radionuclides was mixed with distilled water to a concentration of one-tenth Maximum Permissible Concentration for water (MPC_w) and cycled through the detector cavity. The response of the monitor was noted as a function of gain at a fixed discriminator bias setting.

Plots of monitor counts per minute per 0.1 MPC_w as a function of relative gain determined the gain setting that would allow the greatest variation in relative concentrations of the tested radionuclides while giving the most accurate measure of G.I. tract dose rate. The monitor has a linear response at sample concentrations from 0.001 MPC_w to 10 MPC_w for the above isotopes.

The monitor was calibrated for a number of additional radionuclides

including ^{140}La, ^{106}Ru, ^{103}Ru, ^{131}I, ^{58}Co, ^{69m}Zn, ^{72}Ga, ^{54}Mn and ^{56}Mn, ^{46}Sc and ^{141}Ce. With the exception of ^{131}I, the performance of the monitor was not adversely affected by any of these isotopes.

A G.I. tract dose equivalent measurement of one millirem per month is possible with an accuracy of ±1 mrem, if ^{131}I is not present. The accuracy when ^{131}I is present is a function of the iodine concentration and the total activity of the other radioisotopic present.

DISTRIBUTION

Number of Copies

272 Division of Technical Information Extension

135 Battelle-Northwest

W. J. Bair
C. A. Bennett
W. J. Clarke
R. F. Dickerson
R. J. Engelmann
J. J. Fuquay
R. F. Foster
W. A. Haney
E. R. Irish
R. L. Junkins
D. R. Kalkwarf
A. R. Keene
H. A. Kornberg
W. H. Matchett
R. E. Nakatani
C. E. Newton

Battelle-Northwest (Contd)

J. M. Nielsen
R. F. Palmer
J. L. Palotay
H. M. Parker
R. S. Paul
D. W. Pearce
R. W. Perkins
W. C. Roesch
P. T. Santilli
L. C. Schwendiman
C. L. Simpson
W. A. Snyder
M. F. Sullivan
R. C. Thompson
C. M. Unruh (100)
W. E. Wilson
D. C. Worlton
Technical Information Files (2)
Technical Publications